

Computational Modeling of Transition Temperatures in Spin-Crossover Systems

Jordi Cirera and Eliseo Ruiz

Departament de Química Inorgànica i Orgànica and Institut de Recerca de Química Teòrica i Computacional, Universitat de Barcelona,
Diagonal 645, 08028 Barcelona, Spain

Abstract

A survey of different computational approaches to compute thermochemical properties and, in particular, transition temperatures ($T_{1/2}$) in spin-crossover (SCO) systems is presented. Besides from the possibility of computing accurate values, this work centers its efforts in the use of such computational tools to explain trends in different families of SCO systems, aiming to understand the impact that chemical modifications (both electronic and steric) have over the ligand-field around the metal center, and how such effects can tune the corresponding $T_{1/2}$. By using concepts from molecular orbital theory combined with the results from the calculations, a simple yet accurate depiction of the shift in $T_{1/2}$ can be explained, which enables the rational design of new SCO systems with tailored properties.

Keywords: Spin-crossover, thermochemistry, transition temperature, transition metals.

1. Introduction

Since their discovery, nearly a century ago by Cambi and co-workers,¹ spin-crossover systems have been the focus of intense research due to their inherent technological applications as molecular level switches. Such phenomena, firstly reported as just an experimental observation,¹ found a theoretical background once molecular orbital theory was applied to transition metal complexes, showing that once a metal center is surrounded by ligands, its d-based molecular orbitals must split in different subsets.^{2,3} If the splitting between subsets of d orbitals is large compared to the so-called pairing energy (i.e., the extra interelectronic repulsion resulting from two electrons occupying the same orbital, combined with a lower exchange energy associated with electron pairing), a “low-spin” situation is expected as the ground state. Opposite to that, if the splitting is small compared to the pairing energy, a “high-spin” state should be the most stable one. In some cases though, both effects balance each other, allowing states with different spins to have similar electronic energies. In such cases, the two spin states become accessible and the spin-crossover phenomenon may appear. This situation is illustrated for the very well-known case of an hexacoordinated transition metal complex in an octahedral environment with six purely σ -donor ligands (Figure 1). For that specific case, the five d-orbitals split into two subsets, a triple-degenerate set of non-bonding orbitals (d_{xz} , d_{yz} and d_{xy} , with t_{2g} symmetry) and a two-fold degenerate set of antibonding orbitals ($d_{x^2-y^2}$ and d_{z^2} , with e_g symmetry).⁴ In such case, metals with electronic configurations d^4 to d^7 have access to two alternative spin-states, and if the ligand field generates the right splitting, both states can become thermally accessible.^{5,6} This transition is mostly induced by increasing the temperature over the sample, this is, thermal spin-crossover,⁷ although other external stimulus, such as pressure or electromagnetic radiation can also trigger such property.

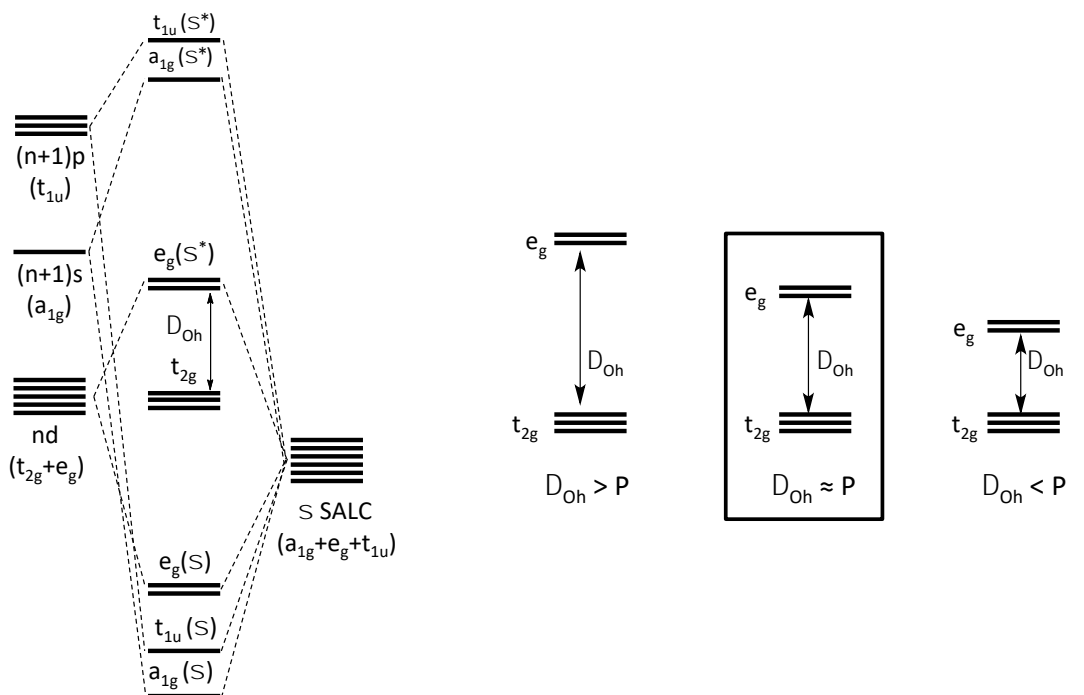


Figure 1: Left, molecular orbital diagram for a six-coordinated octahedral compound with only s-donor ligands, showing the splitting of the five d orbitals into two subsets. Right, splitting of the d-orbitals in strong, medium and weak fields compared with the interelectronic repulsion (P). Intermediate fields will lead to spin-crossover behavior.

For a thermally induced transition to occur, one needs to provide with enough temperature so entropy favors the high-spin situation by overcoming the enthalpic contribution to the Gibbs free energy. This situation is commonly observed in Fe^{II} hexacoordinated complexes with N-donor ligands, but the massive developments in the field have reported many examples of other transition metals exhibiting such behavior, with different coordination numbers, different oxidation states and, of course, different sets of donor atoms. Due to the different occupation of non-bonding and antibonding orbitals between the two alternative spin-states, the transition introduces major changes in the optical, vibrational, magnetic and structural properties of the molecule, thus making SCO molecules perfect candidates for molecular level switching applications. This transition can be monitored with a wide range of physical methods, being the most

common magnetic susceptibility measurements, but many others can be used as well.⁸ From all these measurements, one can plot the molar fraction of each spin-state as a function of the temperature, obtaining the corresponding spin-crossover curve, which allows to measure experimentally the transition temperature ($T_{1/2}$), which is defined as the temperature with equal populations of both spin-states. This parameter, which is key in the physical characterization of SCO systems, is difficult to adjust from the experimental point of view, and its final value is, in most cases, achieved by serendipity.

For that reason, insight from the theoretical point of view will be of great help in rationalizing experimental trends that have been observed, including electronic, steric or both effects simultaneously, in order to foresee how a given system can be modified so its transition temperature raises or decreases. However, computing transition temperatures is a challenging problem, due to the intrinsic difficulty that lays on computing accurately electronic energy differences, a key quantity in SCO systems. In this work, we will introduce the different computational tools that can be used to compute thermochemical quantities, and, as consequence, $T_{1/2}$, surveying the different computational methodologies that have been used so far to address such problem. On a second part, applications to selected examples will be discussed showing how electronic structure calculations can be used to not only compute $T_{1/2}$, but also to rationalize its behavior in terms of the electronic structure of the studied systems, which in turns enables the rational tuning of such property. Finally, conclusions and outlook will be presented.

2. Computing Thermochemistry in Spin-Crossover systems

Spin-crossover appears in systems for which different electronic states (i.e., different spin) have similar energies. In such cases, entropy favors the high-spin state, and a transition from the low-spin to the high-spin state may appear.⁹ Using the thermodynamic description of the spin-crossover process, one can describe such phenomena as an equilibrium between the low-spin (LS) and the high-spin (HS) states. In such case, an assuming and ideal system in which the spin-crossover system is isolated, and neglecting the small pressure-dependent term contribution to the free enthalpy, we can write the corresponding Gibbs energy change (ΔG) for the spin-transition as,^{10,11}

$$\Delta G(T) = G^{HS} - G^{LS} = \Delta H - T\Delta \quad [1]$$

where

$$G^i = H^i - TS^i = E_{el}^i + E_{vib}^i - TS^i \quad [2]$$

is the Gibbs free energy corresponding to spin-state i at the temperature T . In equation [2], the enthalpy term (H^i) includes both electronic (E_{el}^i) and vibrational (E_{vib}^i) contributions. For molecular systems, E_{vib}^i can be properly estimated using the harmonic approximation, while the term E_{el}^i , corresponding to the electronic energy of the spin-state i , can be obtained directly from *ab initio* calculations. The entropy contribution to the free energy (S^i) can also be properly estimated using the harmonic approximation. The Gibbs free energy can be expressed also in terms of the equilibrium constant, K_{eq} , which in turn can be written in terms of the molar fraction of each spin-state,

$$\Delta G(T) = -RT \ln K_{eq} = -RT \ln \frac{\gamma_{HS}}{\gamma_{LS}} = -RT \ln \frac{\gamma_{HS}}{1 - \gamma_{HS}} \quad [3]$$

where R is the gas constant and T the temperature. It is worth mentioning that both ΔH and ΔS have some temperature dependence that can be, in principle, neglected without losing accuracy.^{7,12} By rearranging terms in equation [2], the Gibbs free energy change can be expressed as,

$$\Delta G(T) = \Delta H - T\Delta S = \Delta E_{elec} + \Delta H_{vib} - T\Delta S \quad [4]$$

in which the energy difference between the two electronic states (ΔE_{elec}) is explicitly written. As mentioned above, the vibrational part can be properly computed within the harmonic approximation. Therefore, the remaining term (ΔE_{elec}) is the key quantity to properly model any thermochemical magnitude. In the following sections we will discuss the different theoretical approximations to compute such quantity.

2.1 Density Functional Methods

Due to its balance between computational cost and accuracy,¹³⁻¹⁵ Density Functional Theory (DFT)^{16,17} calculations are currently the most widely used electronic structure method to study molecular systems. Despite its success and its accurate performance towards certain properties, such as vibrational frequencies,¹⁸ it is well known that DFT struggles when it comes to study systems in which major changes in the electronic structure occur, as is the case of SCO molecules. Such systems are very sensitive to the description of the exchange-correlation, which makes up a largest portion of the correlation energy, and therefore the choice of functional becomes a very sensitive issue when targeting electronic energy differences. Despite its limitations, the use of DFT methods to study SCO systems is really appealing.

Over the last years, major efforts have been made in order to use DFT methods to study SCO systems. By reducing the amount of Hartree-Fock exchange to 15%,

Reiher developed the B3LYP* functional, that provides with an accurate description of the SCO behavior for the $[\text{Fe}(\text{phen})_2(\text{NCS})_2]$ complex,^{19,20} and has also been used to study the magnetic properties of the $[\text{Fe}(\text{N}_\text{HS}_4)]\text{L}$ family ($\text{N}_\text{HS}_4 = 2,2\text{-bis}(2\text{-mercaptophenyl-thio)diethylamino}$, $\text{L} = \text{CO}, \text{NO}^+, \text{PR}_3, \text{NH}_3,$ and N_2H_4). By combining Handy's OPTX²¹ exchange functional with the LYP²² and PBE²³ correlation functionals, the OPBE and OLYP methods have shown also good performance towards Fe^{II} SCO systems.^{24,25} The OPBE functional has also shown good performance when it comes to study $[\text{Mn}(\text{Cp}^\text{R})_2]$ ($\text{R} = \text{Me}, ^i\text{Pr}$ or ^tBu) sandwich type systems.²⁶ These methods have recently been tested towards a large dataset of SCO mononuclear molecules, validating one more time its performance.²⁷ That same work proposes the use of the long-range corrected version of the B3LYP functional,²⁸ CAMB3LYP,²⁹ and a modified version of the original functional with a reduced 17% of Hartree-Fock exchange (CAMB3LYP-17) as good candidates to study SCO molecular systems. Similarly, Fe^{II} SCO compounds have also been successfully studied using double hybrid functionals, in particular, the B2PLYP method.³⁰ More recently, the use of the TPSSh^{31,32} functional has proven to be the more general approach to study SCO systems not only based on Fe^{II},^{33,34} but also expanding its use to all metals exhibiting such property on the first transition metal row, this is, Cr^{II}, Mn^{II}, Mn^{III}, Fe^{II}, Fe^{III} and Co^{II}.³⁵ In particular, the TPSSh functional combined with a triple- ζ basis set with polarization functions on all atoms correctly predicts the ground state for a large dataset of SCO systems, and its mean average error when comparing against the experimental $T_{1/2}$ has been estimated in 3.7 kcal/mol, so far, the best result for such type of calculations.³⁶ The effect of dispersion correction using the D3 scheme, zero-point energy vibration and scalar relativistic effects on the computed electronic energy differences was also evaluated at the same level of theory. For most cases, while zero-point energy

correction reduces the gap between both spin-state, relativistic effects have the opposite effect. Despite its versatility, it is worth stressing that specific cases may require specific functionals or reparameterizations if more quantitative results are desired.

It is well known that crystal packing effects, as well as the presence of different types of counterions can lead to different degrees of tuning in the shape of the SCO curve, and eventually even suppressing such behavior for some systems. Therefore, ideally one would like to be able to include such effects, but in practice, the computational cost of computing the vibrations in solid state is huge, and often unaffordable. However, even if this final step could not be achieved, electronic structure calculations with periodic boundary conditions have been carried out in SCO systems using DFT methods, and provide with valuable insight into the behavior of such species. In particular, periodic calculations using the PBE functional with the Hubbard U-term³⁷ have been benchmarked against CASPT2 calculations for several [Fe^{II}N₆] SCO systems.³⁸ Such calculations provided with a U value for the studied systems in the range of 2.37 eV to 2.97 eV (average of 2.65 eV), which turns out to be a good starting point to compute electronic enthalpy changes (i.e, ΔE_{elec}). Additionally, such calculations can also include dispersion corrections, aiming to provide with an accurate depiction of the different effects at play in the crystal structure.

2.2 Wave Function Methods

As stated in equation [4], the key quantity when modeling SCO systems is the electronic energy difference (ΔE_{elec}) between the two alternative spin-states. Regular CASSCF calculations are not really accurate for such type of calculations, because they miss a large portion of the dynamic correlation. Therefore, accurate calculation of spin-state splitting energies must rely in post-CASSCF calculations, in particular

CASPT2/NEVPT2, and coupled cluster (CC) methodologies. In fact, both CASPT2 and NEVPT2 methods have been benchmarked for computing spin-state energies in transition metals against energy differences obtained with CCSD(T) methods.³⁹ From such work, it is shown that, indeed, CASPT2 is a good method of choice to compute electronic energy differences for systems that are either too large for CCSD(T) calculations or too multiconfigurational. The same calibration was done for the particular case of $[M(\text{NCH})_6]^{2+}$ systems ($M = \text{Fe}^{\text{II}}$ or Co^{II}).⁴⁰ using as a reference value CCSD(T) calculations extrapolated to the complete basis set limit. The results showed one more time that CASPT2 calculations provide with a very good value for the corresponding $\Delta E_{\text{HS-LS}}$. Due to its good performance, CASPT2 methods have been used to study specific SCO systems. Several Fe^{II} and Fe^{III} heme models were computed using such methodology, showing that while results for Fe^{III} are pretty accurate, a systematic error can be observed in the Fe^{II} compounds.⁴¹ The SCO behavior of Ni-porphyrine systems exhibiting SCO has also been studied in detail using CASPT2 calculations, rationalizing the effect that the coordination number has over the presence or absence of SCO behavior in such system.⁴² For that last example, the geometrical survey had to be done at DFT level, due to the computational cost that a similar exploration will have with CASPT2. Similarly, if one wants to compute $T_{1/2}$, will need to rely in the harmonic frequencies computed at DFT level. Luckily, it is well know that vibrational analysis is relatively independent of the choice of functional.^{14,18,43,44} Using this hybrid approach (DFT/CASPT2), the $T_{1/2}$ for several Fe^{II} SCO complexes was computed, in very good agreement with the experimental data.⁴⁵ Finally, just mention that another very interesting application of CASPT2 calculations on SCO systems lays in the possibility of studying the effect of electromagnetic radiation over the SCO properties. This has been studied in detail for the $[\text{Fe}(\text{mtz})_6]^{2+}$, $[\text{Fe}(\text{phen})_3]^{2+}$ and $[\text{Fe}(\text{bipy})_3]^{2+}$ molecules,

providing with mechanistic insight into the intersystem crossing relaxation mechanisms responsible for light-induced SCO behavior in such molecules.⁴⁶

2.3 Force-Field Methods

Force-field methods offer the possibility of performing calculations with very rapid execution times, but when dealing with transition metal systems, and, in particular, with systems with more than one electronic state, several problems may appear.⁴⁷ Despite such drawbacks, these methods have been applied to coordination compounds and used to compute several properties for such complexes.⁴⁸ An extremely elegant way to overcome such problems is the use of Ligand-Field Force-Fields (LF-FF), which builds up upon the Angular Overlap Model (AOM),⁴⁹ in the so-called Ligand-Field Molecular Mechanics (LF-MM) scheme. This approach parameterizes the splitting of the d-orbital manifold using metal-ligand distance dependent functions. These functions are used to describe the different AOM parameters that describe σ - and π - type bonding interactions.⁵⁰ Thanks to the latest development in high-level theory calculations, such parameters can nowadays be calculated with high-accuracy using multi-reference *ab initio* methods, such as N-electron valence perturbation theory (NEVPT2).⁵¹ As a result, Deeth and co-workers have used this methodology to study the $[\text{Fe}(\text{bpp})_2]^{2+}$ (bpp=2,6-di(pyrazol-1-yl)pyridine) SCO system and related complexes.⁵² The approach nicely reproduces crystal structures for both spin states, including effects that derive from the use of different counterions, but lacks some precision when computing transition temperatures, because electronic effects have to be yet explicitly incorporated into the LF-MM methods.

3. Applications

From the above, it is clear that computational tools can be used to investigate the behavior of the transition temperature ($T_{1/2}$) in different families of spin-crossover systems, trying to rationalize the shifts that such property experiences on the basis of the local electronic structure, this is, the d-based molecular orbitals. This is key in the design of new SCO systems with tailored properties. In the following section we will discuss several examples, showing how electronic and steric effects, among others, can tune the $T_{1/2}$ for several families of SCO systems.

3.1 Electronic tuning of the $T_{1/2}$

Spin-crossover is, as its core, an electronic structure effect. Once a metal is surrounded by a set of ligands, the d-orbitals split into several subsets. For the iconic octahedral case, this leads to the very well known 3+2 pattern (t_{2g} - e_g). The magnitude of that splitting between these subsets controls the presence or absence of SCO behavior. However, the fine-tuning of these energy gaps in order to control the transition temperature remains elusive. A nice example of how calculations can help understanding the experimental data is provided by the analysis of the *trans*-[Fe(stpy)₄(NCX)₂] (X = S, Se or BH₃) family of ligand-driven light-induced spin-change systems (LD-LISC).⁵³⁻⁵⁵ These systems exhibit an increasing $T_{1/2}$ as a function of the axial ligand strength, nicely following the spectrochemical series. Electronic structure calculations at DFT level using the TPSSh functional provide with an explanation of such behavior in terms of the relevant d-based molecular orbitals.³³ For that particular case, the key interaction in controlling the energy gap is the presence of π -type orbitals in the axial ligands. Such orbitals can interact with the formerly non-bonding pair of orbitals d_{xz} and d_{yz} , generating a bonding and anti-bonding

combinations with the ligands orbitals, and thus leading to different energy gaps as a function of the X atom. In Figure 2, a schematic representation of such effect is illustrated, together with the corresponding d_{xz} orbital for each system. Using equation [3], an estimation of the $T_{1/2}$ for each system can be done, which nicely reproduces the experimental trend, overestimating the experimental values by only 57 K (average).

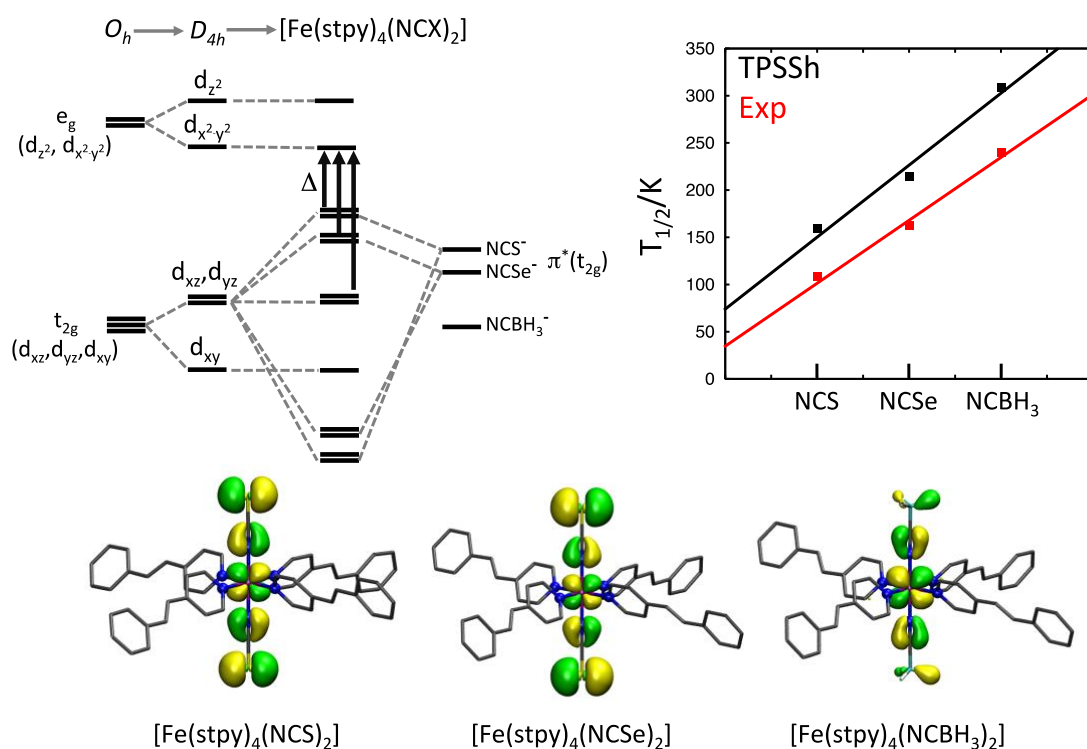


Figure 2: Top-left, schematic representation of the π^* orbitals effect on the axial ligand over the splitting of the d-based MOs on the family of $[Fe(stpy)_4(NCX)_2]$ ($X = S, Se$ or BH_3), showing the increasing splitting (Δ) among the orbitals due to the axial ligand. Top-right, comparison between the computed (TPSSh) and experimental $T_{1/2}$. Bottom, isosurfaces of the d_{xz} orbital, showing the decreasing antibonding character of such orbital with the NCX group.

Another example of how electronic effects tune the $T_{1/2}$ is provided by the analysis of the $[Fe(bpp^{X,Y})_2]^{2+}$ family ($bpp = 2,6$ -di{pyrazol-1-yl}pyridine, $X =$ pyridyl substituent, $Y =$ pyrazolyl substituent). In this case, the correlation between the

electron-donating or electron-attracting character of the X/Y substituent against the computed electronic energy differences between the high-spin and low-spin state ($\Delta E_{\text{HS-LS}}$) using the BP86 functional, showing that it is possible to tune up or down the $T_{1/2}$ in a very gradual manner by proper functionalization of the ligand. Moreover, this effect can be traced back to the d-MOs splitting. A detailed analysis of the strength of each effect on the different subsets of MOs as well as the effect on stabilizing each spin-state was carefully outlined in the study.⁵⁶ Although experimental correlations between $\Delta E_{\text{HS-LS}}$ and the experimental transition temperatures can be obtained, no *ab initio* computed $T_{1/2}$ were reported in this work. The same molecule has been studied from another point of view, trying to understand the role of the counterion in the presence (BF_4^-) or absence (ClO_4^-) of SCO behavior.⁵⁷ Using PBE+U ($U = 2.5$ eV) electronic structure calculations, optimizations of the unit cell with different counterions was done, determining the most stable polymorph for each spin-state in each case, underpinning the thermodynamic and kinetic effects that control each phase transition. The kinetic trapping of the high-spin state for the $[\text{Fe}(\text{bpp})_2](\text{ClO}_4)_2$ systems is explained on the basis of the regular structure of the high-spin polymorph. The authors also shown that similarly to the above indicated, the electronic energy differences can be corrected with the numerical frequencies computed using finite differences, thus allowing for the calculation of the corresponding $T_{1/2}$ for the $[\text{Fe}(\text{bpp})_2]^{2+}$ molecule. The results are in very good agreement with the experimental data.⁵⁷ Similarly, the effect of solvent intermolecular interactions over the crystal packing effects and its implications on the SCO behavior have been modeled for the $[\text{Fe}(\text{E-dpsp})_2](\text{BF}_4)_2 \cdot \text{X}$ ($\text{X} =$ solvent molecule, dpsp = 2,6-bis(1H-pyrazol-1-yl)-4-styrylpyridine) using a PBE+U+D2 methodology.⁵⁸ Although these type of calculations can eventually model the $T_{1/2}$, extracting general trends still challenging due to the computational cost of the numerical frequencies,

which in turn, can only be calculated for the isolated molecule, and not for the entire crystal.

A similar analysis can be extended to dinuclear systems. In such systems, the transition from the low-spin/low-spin state ([LS-LS]) to the high-spin/high-spin state ([HS-HS]) can take place on single step, or via a two-step process, which implies the presence of an intermediate high-spin/low-spin ([HS-LS]) species. It has been previously reported that the presence or absence of a two-step transition can be related to the energy stabilization of the [HS-LS] spin-state relative to the halfway point of the total enthalpy change between the [HS-HS] and the [LS-LS] states.⁵⁹⁻⁶¹ Using the TPSSh functional, the family of $[\text{Fe}(\text{bt})(\text{NCX})_2]_2(\mu\text{-bpym})$ and $[\text{Fe}(\text{pypzH})(\text{NCX})]_2(\mu\text{-pypz})_2$ ($\text{X} = \text{S}, \text{Se}$ and BH_3 , $\text{bt} = 2,20\text{-bi-2-thiazoline}$, $\text{bpym} = 2,20\text{-bipyrimidine}$, $\text{pypzH} = 2\text{-pyrazolylpyridine}$) SCO was analyzed to study the stability of the [HS-LS] state and its implications on the presence or absence of a two-step transition. In Figure 3, the computed change in the magnetic moment, value that can be estimated from the relative populations of each spin-state, against the temperature for the $[\text{Fe}(\text{bt})(\text{NCS})_2]_2(\mu\text{-bpym})$ and $[\text{Fe}(\text{pypzH})(\text{NCSe})]_2(\mu\text{-pypz})_2$ systems is shown, in excellent agreement with the experimentally reported behavior. Calculations shown that, indeed, for the $[\text{Fe}(\text{bt})(\text{NCS})_2]_2(\mu\text{-bpym})$ system, the enthalpy change from the [LS-LS] to the [HS-LS] states lays below the midpoint for the [LS-LS] to [HS-HS] enthalpy change. Therefore, the intermediate state is electronically stabilized, and a two-step transition is observed. In contrast, for the $[\text{Fe}(\text{pypzH})(\text{NCSe})]_2(\mu\text{-pypz})_2$ molecule such value is above the midpoint, thus leading to no stabilization of the intermediate spin state, and leading to a single step transition. A close inspection of the Fe binding pockets using Continuous Shape Measures (CShM)^{62,63} revealed that upon the spin-state change of one of the metal centers, the other binding pocket remains pretty much identical, thus removing

any ligand effect on the control of the two-step transition in these systems, and proving its electronically origin. In fact, a systematic study of the electronic tuning in both systems via modification of the NCX group (X = S, Se or BH₃) shown that increasing the ligand field around the metal center shifts the T_{1/2} to higher values, as expected, but also that larger ligand fields destabilize the [HS-LS] spin-state, thus smoothing the two-step transition to the point that becomes a single-step transition.⁶⁴ For that dinuclear case, the computed T_{1/2} differ more from the experimental values (average of 144 K) than in the above case, but still agree with the experimentally observed trends and provide with a very reasonable estimation of the experimental value.

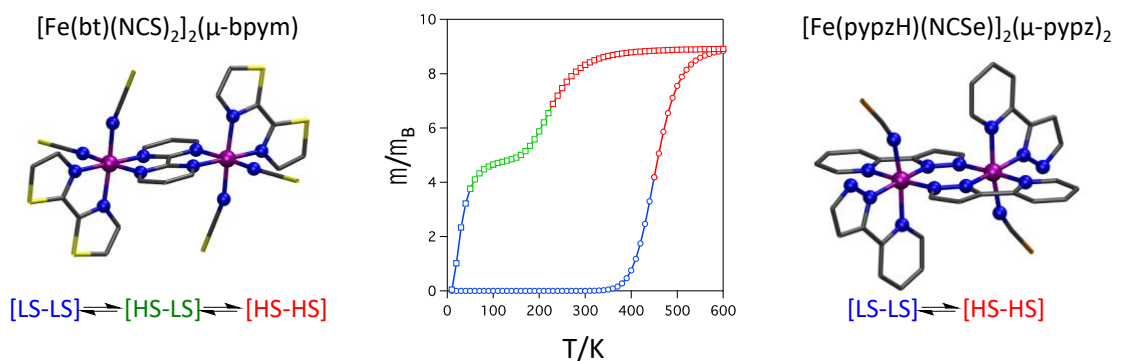


Figure 3: Calculated magnetic moment (μ) for the [Fe(bt)(NCS)₂]₂(μ-bpym) and [Fe(pypzH)(NCSe)₂]₂(μ-pypz)₂ systems, showing the two-step vs. one-step transitions in excellent agreement with the experimentally reported data. Blue for the [LS-LS], green for the [HS-LS] and red for the [HS-HS] spin-states.

Of course, one can explore higher nuclearity systems, but the bigger the system, the more complex the system, the more difficult is to analyze or entangle the different effects at play. Non the less, Borshch and co-workers have been working on the electronic structure study using density functional methods of tetranuclear Fe^{II} SCO molecules, although no modeling of the T_{1/2} in such systems has been yet reported.⁶⁵⁻⁶⁷

3.2 Steric tuning of the $T_{1/2}$

The splitting of the d-based MOs, and therefore $T_{1/2}$, can also be tweaked using ligands of different size, that ultimately control the strength of the metal-ligand bond via steric hindrance. This effect was nicely studied in the family of $[\text{PhB}(\text{MesIm})_3\text{FeNPR}_1\text{R}_2\text{R}_3]$ (Mes = 1,3,5-Trimethylbenzene) reported by Smith and co-workers.⁶⁸ Among the many interesting features of such complexes, it was shown experimentally that the $T_{1/2}$ exhibits a clear correlation with the Tolman cone angle⁶⁹ of the corresponding phosphine group. In particular, bulkier phosphines lead to smaller $T_{1/2}$. The analysis of the electronic effects that control such tuning were analyzed using DFT calculations with the TPSSh functional. One of the more striking features of the studied systems is the fact that a tetracoordinated Fe^{II} metal center could exhibit spin-crossover, when usually the ligand-field splitting for such coordination number is much smaller than the one corresponding to the hexacoordination, thus leading to high-spin systems. The SCO behavior can be explained on the combination of two effects over the ligand field of the metal center. First, there is a strong umbrella distortion introduced by the tridentate ligand, which opens the L-M-L angles from the ideal 109.47° value to an average value of 127.13° . This molecular “folding” generates a splitting of the d-based molecular orbitals that, while decreasing the antibonding character on the d_{xy} and $d_{x^2-y^2}$ orbitals, increases the antibonding character of the d_{xz} and d_{yz} orbitals, therefore, increasing the energy gap between the now formally “non-bonding” orbitals and the antibonding orbitals. Second, the $\{\text{NPR}_1\text{R}_2\text{R}_3\}^-$ ligand increases the antibonding character of the d_{xz} and d_{yz} orbitals via π -antibonding interactions with the pair of orbitals. The net effect is that while having a tetracoordinated system from the coordination point of view, the d-orbital splitting for these molecules is closer the one exhibited by hexacoordinated compounds (Figure 4).

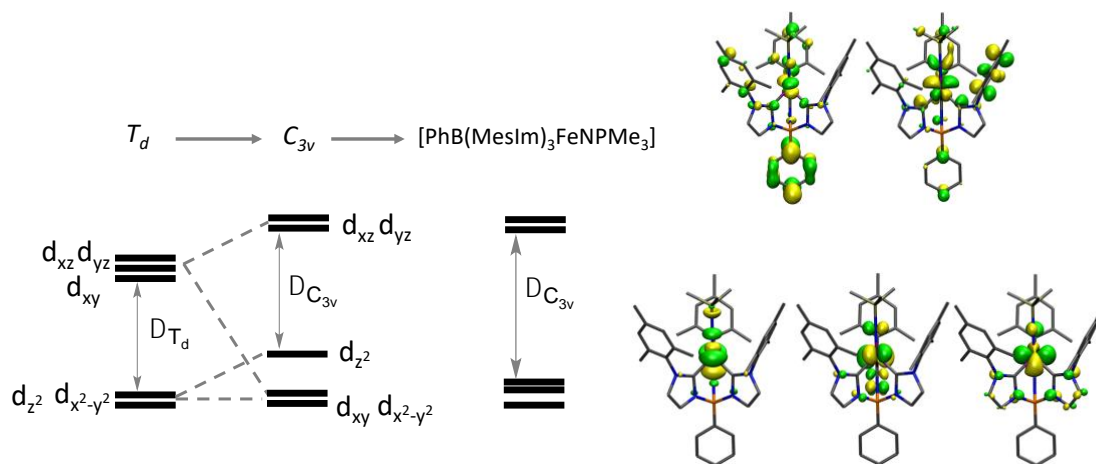


Figure 4. Left, combined effect of the umbrella distortion and the negative charge on the $\{\text{NPR}_1\text{R}_2\text{R}_3\}^-$ ligand over the splitting of the d-orbitals for the $[\text{PhB}(\text{MesIm})_3\text{FeNPR}_1\text{R}_2\text{R}_3]$ family. Right, molecular orbital diagram for the $[\text{PhB}(\text{MesIm})_3\text{FeNPMMe}_3]$ ($S = 0$) molecule, displaying the relevant d-based MOs. Hydrogen atoms omitted for clarity.

Once the origin of the SCO behavior is clear, understanding the tuning of the $T_{1/2}$ becomes the next step. Using the TPSSh functional, the $T_{1/2}$ for all experimentally reported systems was computed, as well as for some members that have not been yet reported.³⁴ The agreement with the experimental data is excellent (average error of only 35K), and the experimental trend is properly reproduced, this is, bulkier phosphines leading to smaller $T_{1/2}$ (figure 5). The origin of such effect lays at the Fe-C interaction. As can be seen in figure 3, the antibonding d_{xz} and d_{yz} orbitals have σ -antibonding contribution from the C-donor atoms of the tridentate ligand. If a small phosphine is used, the whole $\{\text{NPR}_1\text{R}_2\text{R}_3\}^-$ ligand can move in to the cavity generated by the $\{\text{PhB}(\text{MesIm})_3\}^-$ ligand, making the Fe-C bond shorter, and increasing the antibonding interaction between the Fe and the C atoms. This effect raises the energy of the d_{xz} and d_{yz} orbitals, leading to larger energy gaps between the d-MOs and, therefore, higher $T_{1/2}$. The opposite happens for bulkier phosphines. In such case, the $\{\text{NPR}_1\text{R}_2\text{R}_3\}^-$

cannot fit into the cavity, effectively pulling out the Fe center and increasing the Fe-C bond length. This effect reduces the antibonding character of the d_{xz} and d_{yz} orbitals, lowering the energy gap between the non-bonding and antibonding orbitals, thus lowering the corresponding $T_{1/2}$. A comparison between the computed and experimental $T_{1/2}$ is shown in Figure 5. Moreover, on the top of the steric effects, it is possible to investigate the fine-tuning of the $T_{1/2}$ via electronic effects. The lowering of the transition temperature by functionalization of the phenyl group in the $[\text{PhB}(\text{MesIm})_3\text{FeNP}(p\text{-X-C}_6\text{H}_4)_3]$ ($X = \text{-H, -Me, -OMe}$) molecules. The experimental trend is once again properly reproduced, with an overestimation of 70K on average, validating the model once again to study electronic effects (Figure 5).³⁴

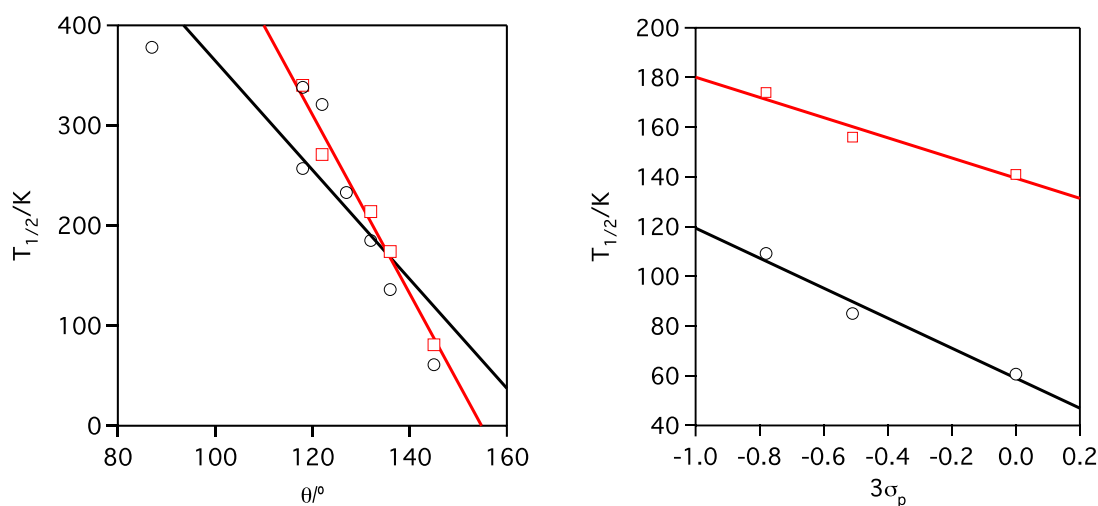


Figure 5. Left, experimental vs. computed $T_{1/2}$ against the Tolman cone angle (θ) for the $[\text{PhB}(\text{MesIm})_3\text{FeNP}R_1R_2R_3]$ family. Right, Experimental vs. computed $T_{1/2}$ for the $[\text{PhB}(\text{MesIm})_3\text{FeNP}(p\text{-X-C}_6\text{H}_4)_3]$ ($X = \text{-H, -Me, -OMe}$) compounds. The computed values (TPSSh) are in black, and the experimental data in red.

3.3 Electronic vs. Steric control of the $T_{1/2}$

As pointed out above, sometimes steric and electronic effects can become competitive and, on the top of that, can affect the transition temperature in different

ways. A nice example of how both effects counterbalance each other is provided by the family of $[\text{Mn}(\text{Cp}^{\text{R}})_2]$ ($\text{R} = \text{Me}, ^i\text{Pr}$ or ^tBu) manganocenes. Experimentally, it is well known that $[\text{Mn}(\text{Cp}^{1-\text{Me}})_2]$ is a spin-crossover molecule, but the $[\text{Mn}(\text{Cp}^*)_2]$, this is, increasing the functionalization of the Cp ring with methyl groups, becomes a low-spin system. On the other hand, functionalization of the Cp ring with bulky substituents (i.e., ^iPr or ^tBu) also removes the SCO behavior, but leads to a high-spin system, which is quite the opposite as before. Therefore, there seems to be a clear competition between both, electronic and steric effects, in controlling not only the transition temperature, but also the SCO properties in such systems. Using DFT calculations with the OPBE functional, an electronic structure study of the $[\text{Mn}(\text{Cp}^{\text{R}})_2]$ family revealed the interplay between both effects.²⁶ Increasing the number of methyl groups, which is an electron-donor group, in the Cp ring, localizes the π -type orbitals that are antibonding towards the d_{xz} and d_{yz} orbitals. This raises the energy of the orbitals, increasing the energy gap between the non-bonding and the antibonding orbitals, which leads to higher $T_{1/2}$ and, eventually, to such a large gap that the system becomes low-spin. In fact, a nice correlation between the number of methyl groups and the $T_{1/2}$ can be outlined, with an average error on the computed $T_{1/2}$ of 111 K. Remarkably, increasing the number of methyl groups barely changes the Cp-Mn metal bond-length, meaning that we are applying solely an electronic effect on the metal's ligand field. Quite the opposite, adding bulky ligands translates in increasing Cp-Mn bond-lengths (around 0.1 Å), which despite the fact that both ^iPr or ^tBu are also electron-donor groups, decreases the antibonding interaction of the Cp ring with the d_{xz} and d_{yz} orbitals, lowering its energy and reducing the energy gap among the d-MOs. This leads to smaller energy gaps, lower $T_{1/2}$ and, eventually, high-spin systems, as experimentally observed. A summary of

both effects is presented in figure 6. Actually, calculations allow to make an estimation of the borderline Mn-Cp distance beyond the one no SCO should be observed.

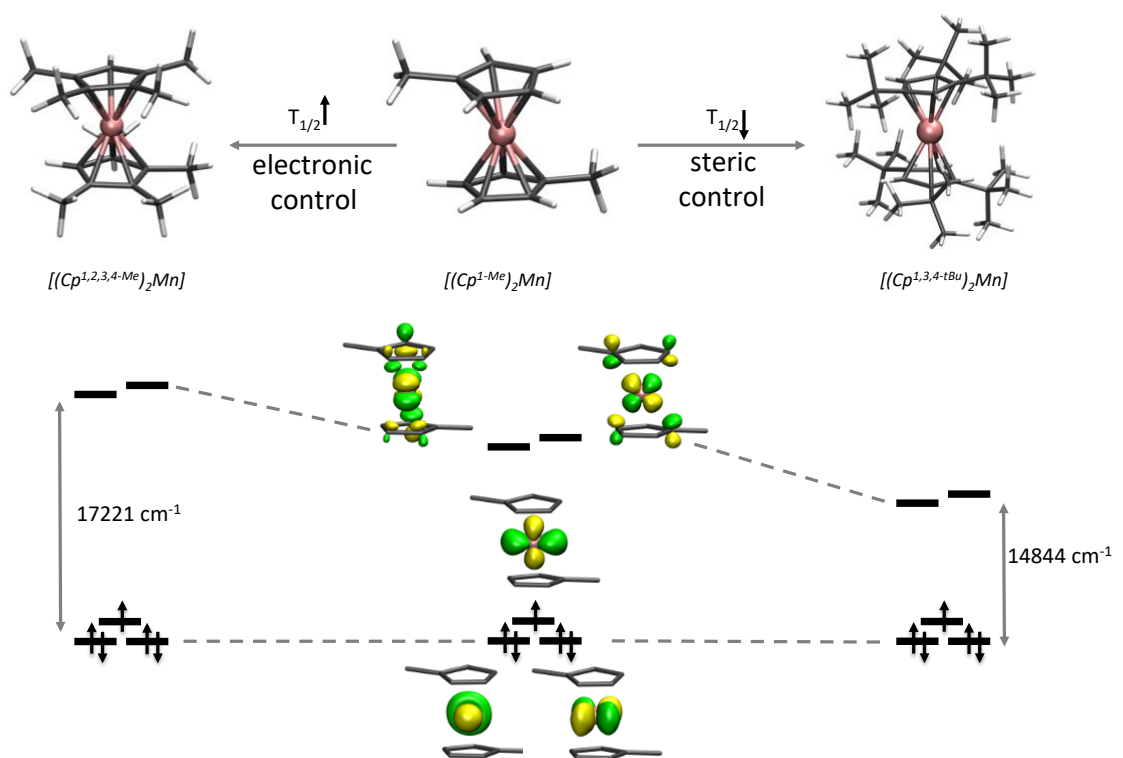


Figure 6: Competitive effects on the control of the transition temperature in the $[\text{Mn}(\text{Cp}^{\text{R}})_2]$ ($\text{R} = \text{-Me, -}^i\text{Pr or -}^t\text{Bu}$) family of SCO systems. Left, electronic control of $T_{1/2}$ by increasing the energy gap between antibonding and non-bonding orbitals via methyl functionalization of the Cp ring. Right, reduction of the same energy gap using bulky substituents ($\text{-}^i\text{Pr or -}^t\text{Bu}$).

3.4 Guest tuning effect of the $T_{1/2}$

A remarkable property of the $\{\text{Fe}(\text{pz})[\text{Pt}(\text{CN})_4]\}$ MOF is that exhibits bidirectional chemo-switching between low-spin and high-spin states upon adsorption of different guest molecules. Specifically, the transition for the empty framework occurs at 295 K with a hysteresis of 24 K ($T_{1/2}(\downarrow) = 285\text{ K}$, $T_{1/2}(\uparrow) = 309\text{ K}$). This transition is strongly affected by the adsorption of protic solvents (e.g., alcohols and water) and bulky molecules (e.g., benzene and pyridine), guest molecules that stabilize the high-

spin state, shifting $T_{1/2}$ to lower values. However, CS_2 molecules adsorbed in the MOF pores stabilize the low-spin state, and some other gases like N_2 seems to have no effect at all. The fact that a key physical property changes upon guest adsorption makes this material a perfect candidate for gas sensing applications.⁷⁰ Using as a starting point the Ligand-Field Molecular-Mechanics (LFMM, section 2.4) approach, an *ab initio* based force field for this MOF was developed and used in a hybrid Monte Carlo/Molecular Dynamics (MC/MD) scheme to study the SCO behavior of such MOF.⁷¹ The same methodology was later used to study the effect of water loading over the $T_{1/2}$ in the material. The results clearly shown that the decrease of $T_{1/2}$ directly correlates with the spatial arrangements of the water molecules inside the pores and the consequent deformation of the framework.⁷² Substantial changes in the MOF are observed a water loadings larger than 3 water molecules per unit cell, forcing the material to expand from the inside, which ultimately results in a progressive stabilization of the high-spin state, with a consequent decrease of $T_{1/2}$ (figure 7). The same methodology was used to study the blocking effect of CS_2 over the SCO behavior. It has been shown that the pyrazine rotational barriers can block the mobility of the guest molecules, confining them to specific regions within the MOF. This confinement makes that the guest molecules significantly slow down the rotational motion of the pyrazine rings which, in turn, leads to the stabilization of the low-spin state by preventing the elongation of the Fe–N bonds of the framework.⁷³

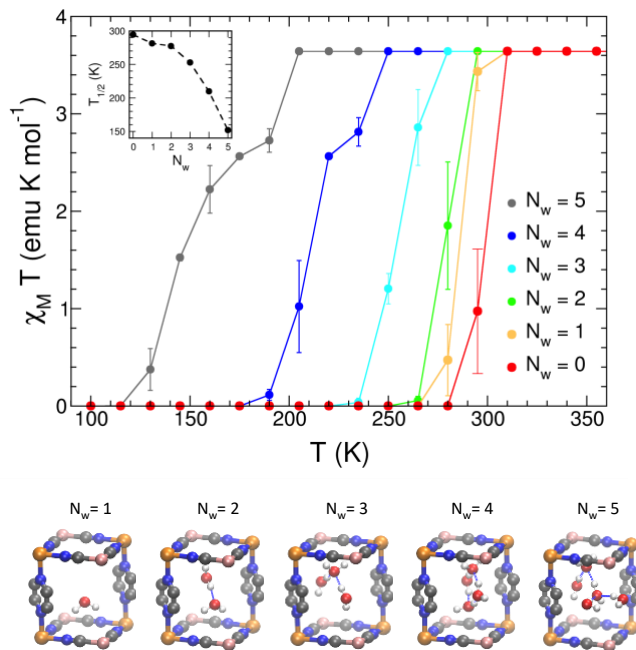


Figure 7: Water loading effect over the $T_{1/2}$ in the $\{\text{Fe}(\text{pz})[\text{Pt}(\text{CN})_4]\}$ MOF. Top, calculated temperature dependence of $\chi_M T$ as a function of the number of water molecules (N_w) per unit cell. Calculated shift in $T_{1/2}$ in the inset. Bottom, water distribution within the pores, showing the water microstructure that forms at higher loadings.

4. Conclusions and Outlook

In this work, we surveyed the different computational approaches that are currently being used to model and intrinsically complex problem, this is, thermochemical quantities in spin-crossover systems, and its applications in the particular case of the transition temperature. The key quantity to accurately compute the change in the free energy that controls the spin transition is the electronic energy difference (ΔE_{elec}) between the two spin-states. Therefore, the quality of the calculations will rely on its accuracy towards this term. Accurate CASPT2 and CC calculations are currently the methods that provide with the best results when computing such quantity, with, obviously, some drawbacks and systematic errors. The performance of such methods has been validated by several authors and for different systems, and there is no

shadow of doubt over the quality of the results. However, the computational cost and expertise required to do such calculations limits its applicability in terms generalizing results or studying families of SCO complexes. Furthermore, if one wants to calculate the corresponding $T_{1/2}$, the vibrational frequencies have to be computed at a lower level of theory, as well as the optimized geometry, being DFT the usual method of choice. In any case, these calculations set up the bar in terms of what is or not a good result for the computed electronic energy difference.

The appealing alternative, this is, the use of DFT to compute not only thermochemical quantities, but also $T_{1/2}$, required a proper benchmarking process towards high level calculations or experimental data. That work reported what, up to day, is the most reliable DFT methodology to study SCO systems. The hybrid meta-GGA functional TPSSh combined with a triple- ζ basis set with polarization functions for all atoms is able to compute ΔE_{elec} with an error of 3.70 kcal/mol when compared with experimental data. This is, so far, the best we can get to broadly address the calculation of thermochemistry associated to SCO, and in order to be more quantitative, one needs to either work out a tailored functional or redo the benchmarking for a given system, both approaches not really appealing from the practical point of view. Thus, this methodology can be used to study several SCO systems belonging to the same family, and used to rationalize the experimentally observed trends in terms of the electronic structure of the studied molecules, which in turn provides with guidelines in the rational design of new SCO systems. This has been used to study the effect of both, electronic effects and steric effects, over the experimental behavior of the $T_{1/2}$, and can be used also to make predictions (as in the case of the $[\text{PhB}(\text{MesIm})_3\text{FeNPR}_1\text{R}_2\text{R}_3]$ family) that are in agreement with the available experimental data, validating its use for the *in silico* screening of new SCO molecules. It is precisely this last point, the possibility of

generalizing trends, what makes such calculations valuable. Using this methodology, the electronic and steric tuning effect over the $T_{1/2}$ can be presented using simple models that correlate the shift in the $T_{1/2}$ with the changes in the ligand field around the metal center in terms of the relevant d-based molecular orbitals. Even if there is a systematic error in the computed values, that simplified picture can be of great help in understanding how chemical modifications affect the physical properties in a given family of SCO systems, which in turns enables the rational design of new molecules with tailored properties.

As indicated above, crystal-packing effects do have an impact in the shape of the spin-crossover curve, enhancing cooperative behavior, or sometimes switching on/off the SCO behavior. Such effects can be modeled by doing periodic electronic structure calculations, and dispersion effects can also be included in the calculations. However, such methods can only be used to calculate electronic energy differences, which is already a big step in including crystal packing effects, but do not grant access to the computed $T_{1/2}$ due to the excessive computational cost that the numerical hessian will have. The alternative to these methods is the use of hybrid molecular mechanics methods using *ab initio* based force fields properly parameterized, which allows the study of condensed phases. This method has proven to be very useful in order to study the effect of different guest molecules and guest loading in the tuning of the $T_{1/2}$ for the specific case of the $\{\text{Fe}(\text{pz})[\text{Pt}(\text{CN})_4]\}$ MOF, providing with an atomistic depiction of the steric effects responsible for the shift towards lower values in $T_{1/2}$ with increasing loadings of water, or the blocking of high-spin state when CS_2 is used as a guest molecule. Even though the construction of such force fields is an expensive job, the results make this approach quite appealing towards the modeling of SCO processes in periodic systems.

We want to stress here that quantitative results for the $T_{1/2}$ may not be possible to reach using a single method. In our experience, some general tools to compute transition temperatures in SCO systems are already available, and allow for the study and rationalization of trends in such systems. However, quantitative results are still a challenge, and it is quite possible that a single method cannot handle everything. Therefore, in order to achieve quantitative results, one must have to combine the best of wave-function methods (CASPT2 or similar, or even higher theory methods) with accurate frequencies at DFT level on a geometry optimized with the most reliable functional for SCO systems. Of course, the inclusion of crystal packing and long-range interactions remains a challenge that cannot be neglected if accuracy is pursued.

In any case, we hope the reader finds the presented discussion useful. We do believe that the main point, this is, the use of computational tools to understand the experimental trends of the $T_{1/2}$ in spin-crossover systems and the possibility of predicting such behavior, appealing and useful towards the design of new molecular devices with tailored properties.

5. Acknowledgements

We thank the Spanish Ministerio de Economía y Competitividad (grant CTQ2015-64579-C3-1-P MINECO/FEDER, UE) and for a Maria de Maeztu grant (MDM-2017-0767).

6. Reference

- (1) Cambi, L.; Szego, L. The magnetic susceptibility of complex compounds. *Ber. Dtsch. Chem. Ges.* **1931**, *64*, 2591-2598.
- (2) Bethe, H. Term Splitting in crystals. *Ann. Phys.* **1929**, *3*, 133-208.
- (3) Van Vleck, J. H. The group relation between the Mulliken and Slater-Pauling theories of valence. *J. Chem. Phys.* **1935**, *3*, 803-806.
- (4) Albright, T. A.; Burdett, J. K.; Whangbo, M. H. *Orbital Interactions in Chemistry*; 2nd ed.; John Wiley & Sons, Inc., 2013.
- (5) *Spin Crossover in Transition Metal Compounds* Gülich, P.; Goodwin, H. A., Eds.; Springer: New York, 2004; Vol. 233-235.
- (6) *Spin-Crossover Materials: Properties and Applications*; Halcrow, M. A., Ed.; John Wiley & Sons: Hoboken, 2013.
- (7) Gülich, P.; Hauser, A.; Spiering, H. Thermal and Optical Switching of Iron(II) Complexes. *Angew. Chem. Int. Ed.* **1994**, *33*, 2024-2054.
- (8) Gülich, P.; Gaspar, A. B.; Garcia, Y. Spin state switching in iron coordination compounds. *Beilstein J. Org. Chem.* **2013**, *9*, 342-391.
- (9) *Spin Crossover in Transition Metal Compounds*; Springer, 2004; Vol. I, II and III.
- (10) Boča, R.; Linert, W. Is there a need for new models of the spin crossover? *Mon. Chem.* **2003**, *134*, 199-216.
- (11) Gülich, P.; Köppen, H.; Link, R.; Steinhäuser, H. G. Interpretation of high-spin reversible low-spin transition in iron(II) complexes .1. Phenomenological thermodynamic model. *J. Chem. Phys.* **1979**, *70*, 3977-3983.
- (12) Paulsen, H.; Schuenemann, V.; Wolny, J. A. Progress in Electronic Structure Calculations on Spin-Crossover Complexes. *Eur. J. Inorg. Chem.* **2013**, 628-641.
- (13) Cohen, A. J.; Mori-Sanchez, P.; Yang, W. Challenges for Density Functional Theory. *Chem. Rev.* **2012**, *112*, 289-320.
- (14) Geerlings, P.; De Proft, F.; Langenaeker, W. Conceptual density functional theory. *Chem. Rev.* **2003**, *103*, 1793-1873.
- (15) Ziegler, T. APPROXIMATE DENSITY FUNCTIONAL THEORY AS A PRACTICAL TOOL IN MOLECULAR ENERGETICS AND DYNAMICS. *Chem. Rev.* **1991**, *91*, 651-667.
- (16) Kohn, W.; Becke, A. D.; Parr, R. G. Density functional theory of electronic structure. *J. Phys. Chem.* **1996**, *100*, 12974-12980.
- (17) Parr, R. G.; Springer Netherlands: Dordrecht, 1980, p 5-15.
- (18) Irikura, K. K.; Johnson, R. D.; Kacker, R. N. Uncertainties in scaling factors for ab initio vibrational frequencies. *J. Phys. Chem. A* **2005**, *109*, 8430-8437.
- (19) Reiher, M. Theoretical study of the Fe(phen)(2)(NCS)(2) spin-crossover complex with reparametrized density functionals. *Inorg. Chem.* **2002**, *41*, 6928-6935.
- (20) Reiher, M.; Salomon, O.; Hess, B. A. Reparameterization of hybrid functionals based on energy differences of states of different multiplicity. *Theor. Chem. Acc.* **2001**, *107*, 48-55.
- (21) Handy, N. C.; Cohen, A. J. Left-right correlation energy. *Mol. Phys.* **2001**, *99*, 403-412.
- (22) Lee, C. T.; Yang, W. T.; Parr, R. G. DEVELOPMENT OF THE COLLE-SALVETTI CORRELATION-ENERGY FORMULA INTO A FUNCTIONAL OF THE ELECTRON-DENSITY. *Phys. Rev. B* **1988**, *37*, 785-789.
- (23) Perdew, J. P.; Burke, K.; Ernzerhof, M. Generalized gradient approximation made simple. *Phys. Rev. Lett.* **1996**, *77*, 3865-3868.

- (24) Güell, M.; Solà, M.; Swart, M. Spin-state splittings of iron(II) complexes with trispyrazolyl ligands. *Polyhedron* **2010**, *29*, 84-93.
- (25) Swart, M. Accurate Spin-State Energies for Iron Complexes. *J. Chem. Theory Comput.* **2008**, *4*, 2057-2066.
- (26) Cirera, J.; Ruiz, E. Electronic and Steric Control of the Spin-Crossover Behavior in (Cp-R)(2)Mn Manganocenes. *Inorg. Chem.* **2018**, *57*, 702-709.
- (27) Siig, O. S.; Kepp, K. P. Iron(II) and Iron(III) Spin Crossover: Toward an Optimal Density Functional. *J. Phys. Chem. A* **2018**, *122*, 4208-4217.
- (28) Becke, A. D. DENSITY-FUNCTIONAL THERMOCHEMISTRY .3. THE ROLE OF EXACT EXCHANGE. *J. Chem. Phys.* **1993**, *98*, 5648-5652.
- (29) Yanai, T.; Tew, D. P.; Handy, N. C. A new hybrid exchange-correlation functional using the Coulomb-attenuating method (CAM-B3LYP). *Chem. Phys. Lett.* **2004**, *393*, 51-57.
- (30) Ye, S.; Neese, F. Accurate Modeling of Spin-State Energetics in Spin-Crossover Systems with Modern Density Functional Theory. *Inorg. Chem.* **2010**, *49*, 772-774.
- (31) Staroverov, V. N.; Scuseria, G. E.; Tao, J. M.; Perdew, J. P. Comparative assessment of a new nonempirical density functional: Molecules and hydrogen-bonded complexes. *J. Chem. Phys.* **2003**, *119*, 12129-12137.
- (32) Tao, J. M.; Perdew, J. P.; Staroverov, V. N.; Scuseria, G. E. Climbing the density functional ladder: Nonempirical meta-generalized gradient approximation designed for molecules and solids. *Phys. Rev. Lett.* **2003**, *91*, 146401.
- (33) Cirera, J.; Paesani, F. Theoretical Prediction of Spin-Crossover Temperatures in Ligand-Driven Light-Induced Spin Change Systems. *Inorg. Chem.* **2012**, *51*, 8194-8201.
- (34) Cirera, J.; Ruiz, E. Theoretical Modeling of the Ligand-Tuning Effect over the Transition Temperature in Four-Coordinated Fe-II Molecules. *Inorg. Chem.* **2016**, *55*, 1657-1663.
- (35) Jensen, K. P.; Cirera, J. Accurate Computed Enthalpies of Spin Crossover in Iron and Cobalt Complexes. *J. Phys. Chem. A* **2009**, *113*, 10033-10039.
- (36) Cirera, J.; Via-Nadal, M.; Ruiz, E. Benchmarking Density Functional Methods for Calculation of State Energies of First Row Spin-Crossover Molecules. *Inorg. Chem.* **2018**, *57*, 14097-14105.
- (37) Dudarev, S. L.; Botton, G. A.; Savrasov, S. Y.; Humphreys, C. J.; Sutton, A. P. Electron-energy-loss spectra and the structural stability of nickel oxide: An LSDA+U study. *Phys. Rev. B* **1998**, *57*, 1505-1509.
- (38) Vela, S.; Fumanal, M.; Ribas-Arino, J.; Robert, V. Towards an accurate and computationally-efficient modelling of Fe(II)-based spin crossover materials. *Phys. Chem. Chem. Phys.* **2015**, *17*, 16306-16314.
- (39) Pierloot, K.; Quan Manh, P.; Domingo, A. Spin State Energetics in First-Row Transition Metal Complexes: Contribution of (3s3p) Correlation and Its Description by Second-Order Perturbation Theory. *J. Chem. Theory Comput.* **2017**, *13*, 537-553.
- (40) Daku, L. M. L.; Aquilante, F.; Robinson, T. W.; Hauser, A. Accurate Spin-State Energetics of Transition Metal Complexes. 1. CCSD(T), CASPT2, and DFT Study of M(NCH)(6) (2+) (M = Fe, Co). *J. Chem. Theory Comput.* **2012**, *8*, 4216-4231.
- (41) Vancoillie, S.; Zhao, H.; Radon, M.; Pierloot, K. Performance of CASPT2 and DFT for Relative Spin-State Energetics of Heme Models. *J. Chem. Theory Comput.* **2010**, *6*, 576-582.
- (42) Alcover-Fortuny, G.; de Graaf, C.; Caballol, R. Spin-crossover in phenylazopyridine-functionalized Ni-porphyrin: trans-cis isomerization triggered by pi-pi interactions. *Phys. Chem. Chem. Phys.* **2015**, *17*, 217-225.

- (43) Frenking, G.; Frohlich, N. The nature of the bonding in transition-metal compounds. *Chem. Rev.* **2000**, *100*, 717-774.
- (44) Siegbahn, P. E. M.; Blomberg, M. R. A. Transition-metal systems in biochemistry studied by high-accuracy quantum chemical methods. *Chem. Rev.* **2000**, *100*, 421-437.
- (45) Rudavskiy, A.; Sousa, C.; de Graaf, C.; Havenith, R. W. A.; Broer, R. Computational approach to the study of thermal spin crossover phenomena. *J. Chem. Phys.* **2014**, *140*.
- (46) Sousa, C.; Llundell, M.; Domingo, A.; de Graaf, C. Theoretical evidence for the direct (MLCT)-M-3-HS deactivation in the light-induced spin crossover of Fe(II)-polypyridyl complexes. *Phys. Chem. Chem. Phys.* **2018**, *20*, 2351-2355.
- (47) Deeth, R. J. The ligand field molecular mechanics model and the stereoelectronic effects of d and s electrons. *Coord. Chem. Rev.* **2001**, *212*, 11-34.
- (48) Comba, P.; Hambley, T. W.; Martin, B. *Molecular Modeling of Inorganic Compounds*; 3rd ed.; Wiley-VCH, 2009.
- (49) Schaffer, C. E.; Jorgensen, C. K. Angular Overlap Model An Attempt to Revive Ligand Field Approaches. *Mol. Phys.* **1965**, *9*, 401-&.
- (50) Deeth, R. J.; Anastasi, A.; Diedrich, C.; Randell, K. Molecular modelling for transition metal complexes: Dealing with d-electron effects. *Coord. Chem. Rev.* **2009**, *253*, 795-816.
- (51) Singh, S. K.; Eng, J.; Atanasov, M.; Neese, F. Covalency and chemical bonding in transition metal complexes: An ab initio based ligand field perspective. *Coord. Chem. Rev.* **2017**, *344*, 2-25.
- (52) Deeth, R. J.; Halcrow, M. A.; Cook, L. J. K.; Raithby, P. R. Ab Initio Ligand Field Molecular Mechanics and the Nature of Metal-Ligand pi-Bonding in Fe(II) 2,6-di(pyrazol-1-yl)pyridine Spin Crossover Complexes. *Chem. Eur. J* **2018**, *24*, 5204-5212.
- (53) Boillot, M. L.; Chantraine, S.; Zarembowitch, J.; Lallemand, J. Y.; Prunet, J. First ligand-driven light-induced spin change at room temperature in a transition-metal molecular compound. *New J. Chem.* **1999**, *23*, 179-183.
- (54) Boillot, M. L.; Roux, C.; Audiere, J. P.; Dausse, A.; Zarembowitch, J. Ligand-driven light-induced spin change in transition-metal complexes: Selection of an appropriate system and first evidence of the effect, in Fe-II(4-styrylpyridine)(4)(NCBPh(3))(2). *Inorg. Chem.* **1996**, *35*, 3975-3980.
- (55) Roux, C.; Zarembowitch, J.; Gallois, B.; Granier, T.; Claude, R. Toward Ligand-Driven Light-Induced Spin Change. Influence of the Configuration of 4-Styrylpyridine (stpy) on the Magnetic Properties of Fe(stpy)₄(NCS)₂ Complexes. Crystal Structures of the Spin-Crossover Species Fe(trans-stpy)₄(NCS)₂ and of the High-Spin Species Fe(cis-stpy)₄(NCS)₂. *Inorg. Chem.* **1994**, *33*, 2273-2279.
- (56) Cook, L. J. K.; Kulmaczewski, R.; Mohammed, R.; Dudley, S.; Barrett, S. A.; Little, M. A.; Deeth, R. J.; Halcrow, M. A. A Unified Treatment of the Relationship Between Ligand Substituents and Spin State in a Family of Iron(II) Complexes. *Angew. Chem. Int. Ed.* **2016**, *55*, 4327-4331.
- (57) Vela, S.; Novoa, J. J.; Ribas-Arino, J. Insights into the crystal-packing effects on the spin crossover of Fe-II(1-bpp) (2+)-based materials. *Phys. Chem. Chem. Phys.* **2014**, *16*, 27012-27024.
- (58) Fumanal, M.; Jimenez-Gravalos, F.; Ribas-Arino, J.; Vela, S. Lattice-Solvent Effects in the Spin-Crossover of an Fe(II)-Based Material. The Key Role of Intermolecular Interactions between Solvent Molecules. *Inorg. Chem.* **2017**, *56*, 4474-4483.

- (59) Ksenofontov, V.; Gaspar, A. B.; Niel, V.; Reiman, S.; Real, J. A.; Gutlich, P. On the nature of the plateau in two-step dinuclear spin-crossover complexes. *Chem. Eur. J* **2004**, *10*, 1291-1298.
- (60) Real, J. A.; Bolvin, H.; Bousseksou, A.; Dworkin, A.; Kahn, O.; Varret, F.; Zarembowitch, J. Two-step spin crossover in the new dinuclear compound [Fe(bt)(NCS)₂]₂bpym, with bt = 2,2'-bi-2-thiazoline and bpym = 2,2'-bipyrimidine: experimental investigation and theoretical approach. *J. Am. Chem. Soc.* **1992**, *114*, 4650-4658.
- (61) Zein, S.; Borshch, S. A. Energetics of binuclear spin transition complexes. *J. Am. Chem. Soc.* **2005**, *127*, 16197-16201.
- (62) Alvarez, S.; Alemany, P.; Casanova, D.; Cirera, J.; Llunell, M.; Avnir, D. Shape maps and polyhedral interconversion paths in transition metal chemistry. *Coord. Chem. Rev.* **2005**, *249*, 1693-1708.
- (63) Alvarez, S.; Ruiz, E. In *Supramolecular Chemistry, From Molecules to Nanomaterials*; Steed, J. W., Gale, P. A., Eds.; John Wiley & Sons: Chichester, UK, 2012; Vol. 5, p 1993-2044.
- (64) Cirera, J.; Ruiz, E. Theoretical modeling of two-step spin-crossover transitions in Fe-II dinuclear systems. *J. Mater. Chem. C* **2015**, *3*, 7954-7961.
- (65) Borshch, S. A.; Zueva, E. M. Theoretical Study of Spin-State and Redox Multistability in an Iron 2x2 Grid Complex. *Eur. J. Inorg. Chem.* **2013**, 1009-1014.
- (66) Zueva, E. M.; Ryabikh, E. R.; Borshch, S. A. Theoretical Analysis of Spin Crossover in Iron(II) 2 x 2 Molecular Grids. *Inorg. Chem.* **2011**, *50*, 11143-11151.
- (67) Zueva, E. M.; Ryabikh, E. R.; Kuznetsov, A. M.; Borshch, S. A. Spin Crossover in Tetranuclear Cyanide-Bridged Iron(II) Square Complexes: A Theoretical Study. *Inorg. Chem.* **2011**, *50*, 1905-1913.
- (68) Lin, H. J.; Siretanu, D.; Dickie, D. A.; Subedi, D.; Scepaniak, J. J.; Mitcov, D.; Clerac, R.; Smith, J. M. Steric and Electronic Control of the Spin State in Three-Fold Symmetric, Four-Coordinate Iron(II) Complexes. *J. Am. Chem. Soc.* **2014**, *136*, 13326-13332.
- (69) Tolman, C. A. Phosphorus ligand exchange equilibria on zerovalent nickel. Dominant role for steric effects. *J. Am. Chem. Soc.* **1970**, *92*, 2956-2965.
- (70) Ohba, M.; Yoneda, K.; Agusti, G.; Munoz, M. C.; Gaspar, A. B.; Real, J. A.; Yamasaki, M.; Ando, H.; Nakao, Y.; Sakaki, S.; Kitagawa, S. Bidirectional Chemo-Switching of Spin State in a Microporous Framework. *Angew. Chem. Int. Ed.* **2009**, *48*, 4767-4771.
- (71) Cirera, J.; Babin, V.; Paesani, F. Theoretical Modeling of Spin Crossover in Metal-Organic Frameworks: Fe(pz)₂Pt(CN)₄ as a Case Study. *Inorg. Chem.* **2014**, *53*, 11020-11028.
- (72) Pham, C. H.; Cirera, J.; Paesani, F. Molecular Mechanisms of Spin Crossover in the {Fe(pz)₂Pt(CN)₄} Metal-Organic Framework upon Water Adsorption. *J. Am. Chem. Soc.* **2016**, *138*, 6123-6126.
- (73) Pham, C. H.; Paesani, F. Guest-Dependent Stabilization of the Low-Spin State in Spin-Crossover Metal-Organic Frameworks. *Inorg. Chem.* **2018**, *57*, 9839-9843.